Resolution, visibility and contrast enhancement in 2D and 3D photoacoustic imaging: a unified approach based on absorption fluctuations analysis

Bastien Arnal, Guillaum Godefroy, Sergey Vilov, Emmanuel Bossy

RESOLUTION, VISIBILITY AND CONTRAST ENHANCEMENT IN 2D AND 3D PHOTOACOUSTIC IMAGING: A UNIFIED APPROACH BASED ON ABSORPTION FLUCTUATIONS ANALYSIS

Bastien Arnal[1] **Guillaume Godefroy**[1] **Sergey Vilov**[1]
Emmanuel Bossy[1]
[1] Univ. Grenoble Alpes, CNRS, LIPhy, 38000 Grenoble, France
bastien.arnal@univ-grenoble-alpes.fr

ABSTRACT

Photoacoustic imaging provides optical contrast at depth beyond the optical transport mean free path. From the generation of ultrasound by light absorption, images can be reconstructed at the acoustic resolution (100 µm) with a penetration of a few cm. Improving the resolution to bring it closer to the cellular scale is a major challenge. Moreover, the design of imaging systems often leads to limited view artifacts, where a part of the information needed for a complete reconstruction of the objects is missing. We studied multiple approaches for improving the resolution, visibility and contrast of photoacoustic imaging. We will show that a dynamic approach based on the analysis of fluctuations induced by a flow of absorbers can significantly improve resolution. The fluctuation approach, which has the advantage to use the native contrast of blood, also solves the visibility problem in 2D imaging of flow phantoms using a linear transducer (128 elements, 15 MHz). We will show this approach is effective using a sparse array of detectors for 3D imaging. Using a sparse spherical array (256 elements, 8 MHz), 3D imaging experiments in the chicken embryo vasculature model evidenced the presence of clutter around the reconstructed objects due to the low number of channels, resulting in a poor contrast. This clutter was greatly reduced by the fluctuation approach. We will further discuss photoacoustic fluctuations and ultrasound power Doppler similarities. Thus, photoacoustic fluctuation imaging overcomes many limitations of conventional imaging and will be further evaluated for in-vivo imaging.

1. INTRODUCTION

Photoacoustic (PA) imaging (PAI) is a biomedical imaging modality that uses the mechanism of light absorption to generate acoustic waves and forms images of optical contrast at depths [1]. In acoustic-resolution PA imaging, arrays of ultrasound detectors are used to collect PA signals. The resulting resolution is on the order of 100 μm. There is a broad interest in achieving super-resolution with PAI [2]. Localization-based techniques can give the highest resolution enhancement but need exogenous agents [3] [4]. Model-based techniques can improve resolution without the use of contrast agents with sparsity and positivity constraints in the reconstruction [5], which poses the problem of determining regularization parameters. Previous studies showed that fluctuations on the PA images provided by random speckle illuminations could be exploited for resolution enhancement [6]. In this work, we will exploit absorption fluctuations provided by the flow of red blood cells, which prevents using contrast agents.

After reconstruction using standard delay-and-sum algorithms, the finite size and the limited-bandwidth of the detectors generate some visibility artefacts. On the resulting image, the vessels having a structure elongated towards the transducer are invisible due to coherent acoustic effects. The inner part of large vessels, presenting low frequency components outside the bandwidth of the transducer are also missing. Various solutions have been proposed to compensate the visibility artefacts such as rotating the ultrasound probe around the object or placing acoustic reflectors at edges of the imaging zone [7] [8]. These methods are not applicable in a clinical environment. We will show how fluctuations provided by the flow of absorbers solves the visibility problem.

Going from 2D imaging to 3D imaging poses engineering issues regarding the number of transducers and their corresponding electronic channels. A few thousands of elements would be needed to achieve a similar image quality as in 2D imaging. To bypass this issue, we used the fluctuation PAI approach and we will show why it also improves the contrast greatly in the imaging of 3D volumes.

2. THEORY

2.1 Fluctuation image

Let's consider a flow of particles uniformly filled with molecular absorbers of absorption μ_0. We aim at imaging vessels given by a binary spatial function $f(\mathbf{r})$. The repartition of flowing particles is given by a fluctuating function $g_k(\mathbf{r})$ that will change among realizations (k). The medium is supposed to be shined uniformly with a constant light fluence F_0. A single PAI reconstructed picture can be expressed as:

$$A_k(\mathbf{r}) = \Gamma F_0 \mu_0 (f(\mathbf{r}) g_k(\mathbf{r})) * h(\mathbf{r}) \qquad (1)$$

where Γ is the Gruneisen coefficient and $h(\mathbf{r})$ is the PSF of the imaging system. If we perform several images, we can

compute the coherent mean value of 2 and take its magnitude:

$$| < A_k(\mathbf{r}) > | = \Gamma F_0 \mu_0 \eta | f(\mathbf{r}) * h(\mathbf{r}) | \qquad (2)$$

where $\eta =< g_k(\mathbf{r}) >$ reprensents the volume fraction of particles or the hematocrit in the case of a blood flow. $< A_k(\mathbf{r}) >$ is the limited-view conventional PA image.

We showed in [9] that the variance image can be expressed as:

$$\sigma[A]^2(\mathbf{r}) = \Gamma^2 \mu_0^2 F_0^2 \sigma_g^2 V_g f^2(\mathbf{r}) * |h|^2(\mathbf{r}) \qquad (3)$$

where σ_g^2 is the variance of the function $g(\mathbf{r})$ and V_g is a volume containing information about the particles volume and their relative correlation in space. Note that this formula applies to continuous absorption or illumination fluctuation profiles (e.g. concentration gradients of molecular absorbers or, speckle illuminations...). For a flow of particles, we can use the well-known packing factor definition $W(\eta)$ [10] to derive an alternative expression:

$$\sigma[A]^2(\mathbf{r}) = \Gamma^2 \mu_0^2 F_0^2 \eta W(\eta) V_p f^2(\mathbf{r}) * |h|^2(\mathbf{r}) \qquad (4)$$

where V_p is the particle volume.

The convolution with $|h|^2(\mathbf{r})$ is the key for visibility enhancement. Eq.2 is a coherent convolution and Eq.3 is an incoherent one. The destructive interference occurring in Eq.2 with the bipolar PSF can no longer happen when convolving with the squared envelope of the PSF. The summations in Eq.3 and Eq.4 can never interfere destructively. In the Fourier spatial domain, $|h|^2(\mathbf{r})$ gains a low spatial frequency part which shows that we can recover objects that are subject to visibility artefacts. For more information, the reader is kindly directed to [9].

2.2 Super-resolution with flow-induced fluctuations

The variance image already has a resolution enhancement of a factor $\sqrt{2}$ compared with conventional PAI. The cumulant K_n is a statistical measure that can be calculated at any order n, from the moments of lower order. We adapted the SOFI (Super-resolution optical fluctuation imaging) theory for PAI [11]. The cumulant image K_n can be expressed as :

$$K_n(\mathbf{r}) \propto [(F_0 \cdot f(\mathbf{r}))^n \cdot K_n(g_k(\mathbf{r}))] * |h(\mathbf{r})|^n \qquad (5)$$

where $K_n(g_k(\mathbf{r}))$ is the cumulant of the fluctuating function $g_k(\mathbf{r})$. As the convolution happens with a sharper PSF function, the n^{th} order cumulant image K_n has a resolution enhancement of $\sqrt{n}$. The imaged quantity $(F_0.f(r))^n$ is also at the n^{th} power which amplifies the dominance of brighter objects. It may be useful to display the linearized cumulant $K_n^{1/n}$ alternatively.

3. METHODS

3.1 Setup and configuration

Our 2D PAI system uses a free space laser beam emitted by a frequency-doubled NAD-YAG laser coupled to an OPO (Innolas, DPSS Spitlight) at the rate of 100 Hz. We use a 15 MHz central frequency linear array (L228v Kolo Medical, Korea) with 128 active channels. The probe is connected to a Vantage 256 High Frequency system (Verasonics, USA). Our 3D PAI system uses the same laser coupled to a fiber bundle (Ceramoptek, Germany) attached at the center of a custom spherical phased array (256 channels, Imasonic, France). The acoustic coupling is performed through a cone where a latex membrane is held tight. Imaging sequences consist in recording a series of frames at 100 Hz frame rate and the RF signals are saved during acquisition. Offline beamforming and postprocessing is then achieved on a regular computer.

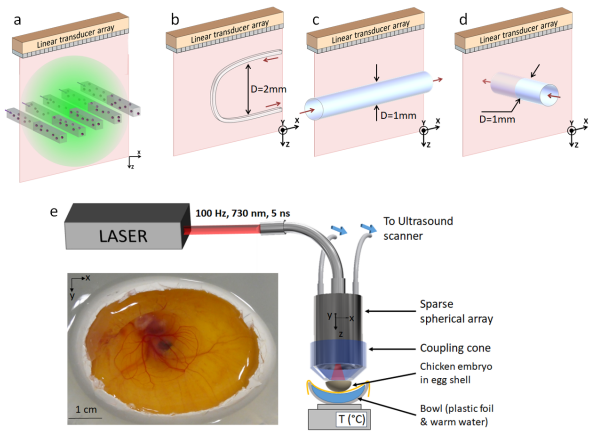

Figure 1. Experimental configurations. a) Super-resolution experiment with microfluidic channels flown by particles. b-d) Visibility enhancement experiments: b) angular visibility enhancement, c-d) Bandwidth visibility enhancement in resp. in-plane and transverse flows. e) 3D setup applied to imaging of chicken embryo

.

3.2 SVD filtering

The estimation of the variance image (or cumulants) is impacted by the pulse-to-pulse energy fluctuation (PEF) of the laser. Removing the mean pixel value over the realizations before integrating is not sufficient to remove the fluctuating contributions of the mean absorber. Therefore, we use an approach employed in Ultrasound doppler called SVD filtering [12]. The first singular vector will contain the temporally varying "mean absorber" which can be then effectively removed. A broad study on the SVD was done in the supplementary materials of [9].

4. RESULTS

We first demonstrate resolution enhancement using microfluidic channels.

4.1 Resolution

10 μm polystyrene beads were flown into a microfluidic circuit composed of 5 equidistant channels represented in

Fig.2a. A series of 4000 images were recorded and reconstructed. The mean image (Fig.2b) do not resolve the 5 channels while they are increasingly distinguishable at 2^{nd}, 3^{rd} and $6^{th} orders$ (see Fig.2c-e). A non-uniform spatial laser intensity induced a non constant value over the 5 channels. At the 6^{th} order, it is required to use the linearized version shown in Fig.2f which interestingly still shows a resolution enhancement with a clear discrimination of the 5 channels, even if the size of each spot is back to the initial first-order resolution.

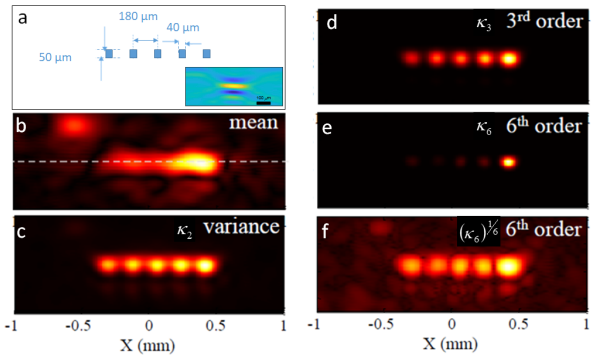

Figure 2. Super resolution fluctuation photoacoustic imaging. a) microfluidic channels dimensions and PSF at the same scale. b) Mean conventional PA image. c-e) Cumulants of orders 2, 3 and 6. f) Linearized 6^{th}-order cumulant.

.

4.2 Visibility

The 3 configurations shown in Fig.1b-d) were realized experimentally by flowing human whole blood in tubes. The mean images in Fig.3$a_1 - c_1$ (as well as single shot pictures, not shown here) clearly show visibility artefacts that vanish when computing the fluctuation image (square root of the variance image) in Fig.3$a_2 - c_2$.

4.3 Visibility and contrast: 3D imaging results

We further evaluate Fluctuation PAI on a live sample in the chicken embryo model. The chorioallantoic membrane is imaged with our 3D imaging system at $730nm$. When imaging with a sparse array (here, only 256 channels applied to 3D imaging), there is a lack of information to have a good reconstruction. As a result, clutter appears on the image background and induces a low constrast as shown in the maximum intensity projection (MIPs) in the top row of Fig.4. Fluctuation images are shown in the bottom row and show both visibility and contrast improvements. Contrast to noise ratio (CNR) is increased from 3.1 to 6.3.

5. DISCUSSION AND CONCLUSION

High-order statistics of these fluctuations led to super-resolution. The most practical use could be the variance image (or standard deviation) since it is straightforward. More work is needed to demonstrate these effects at higher

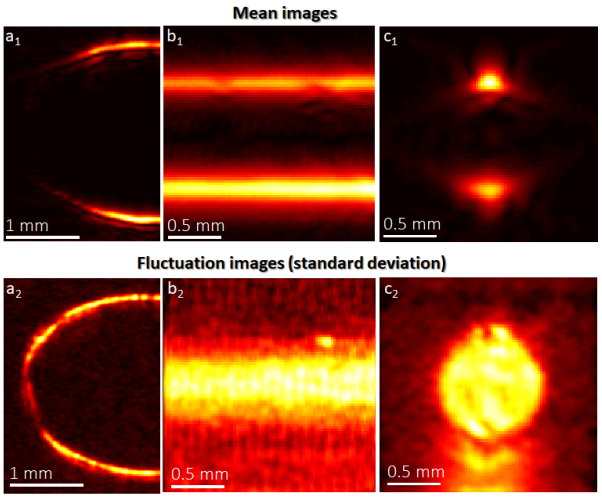

Figure 3. Visibility artefact removal for the experiments b, c and d of Fig.1. Top row Mean conventional images. Bottom row: Corresponding Fluctuation image (standard deviation)

.

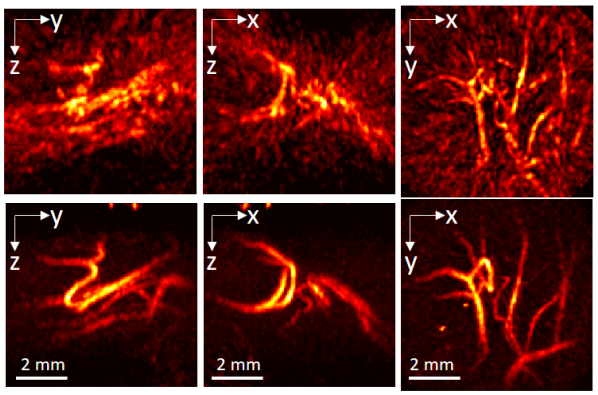

Figure 4. Visibility artefact removal for the experiments b, c and d of Fig1. Top row Mean conventional images. Bottom row: Corresponding Fluctuation image (standard deviation)

.

orders in pratical *in vivo* situations. Moreover, fluctuations also solved the two visibility problems: 1) the directivity of the sources, happening when a source sends all its energy in a direction not covered by the transducer; 2) the spectral content of the sources which concerns sources that are larger than the acoustic central wavelength of the employed transducer. This method is easy to implement on all systems and could impact a number of study allowing to see more structures and features in the vasculature that were previously invisible. Additionally, 3D imaging experiments showed spectacular contrast enhancement with the reduction of clutter. This background noise is much larger for conventional images because coherent side lobe effects are accumulating along spatially coherent absorbers. The incoherence of the fluctuation summation blurs these side

lobes contributions resulting in a much larger CNR. The applicability of this technique is dependent upon quantifying the fluctuations which are typically 1 to 2-orders of magnitude lower than the mean PA signals. The low SNR values is not an intrinsic limitation and can be compensated with a large number of frames as discussed in [9].

In this work, we demonstrated that fluctuations of absorption induced by blood flow could lead to super-resolution, visibility artefacts removal and contrast enhancement. The force of Fluctuation PAI is to overcome these many issues with a non-scanning system that can be handheld and used for navigation in the clinical environment without the use of contrast agents. However, as many other techniques, image enhancement is achieved at the cost of time-resolution since hundreds of images are needed. Alternative approaches such as Deep Learning image enhancement have to compared to it [13] and further *in vivo* in small rodents models.

6. REFERENCES

[1] P. Beard, "Biomedical photoacoustic imaging," *Interface focus*, vol. 1, no. 4, pp. 602–631, 2011.

[2] J. Shi, Y. Tang, and J. Yao, "Advances in super-resolution photoacoustic imaging," *Quantitative imaging in medicine and surgery*, vol. 8, no. 8, p. 724, 2018.

[3] S. Vilov, B. Arnal, and E. Bossy, "Overcoming the acoustic diffraction limit in photoacoustic imaging by the localization of flowing absorbers," *Optics letters*, vol. 42, no. 21, pp. 4379–4382, 2017.

[4] X. L. Dean-Ben and D. Razansky, "Localization optoacoustic tomography," *Light: Science & Applications*, vol. 7, no. 4, pp. 18004–18004, 2018.

[5] S. Vilov, B. Arnal, E. Hojman, Y. C. Eldar, O. Katz, and E. Bossy, "Super-resolution photoacoustic and ultrasound imaging with sparse arrays," *Scientific reports*, vol. 10, no. 1, pp. 1–8, 2020.

[6] T. Chaigne, J. Gateau, M. Allain, O. Katz, S. Gigan, A. Sentenac, and E. Bossy, "Super-resolution photoacoustic fluctuation imaging with multiple speckle illumination," *Optica*, vol. 3, no. 1, pp. 54–57, 2016.

[7] R. A. Kruger, W. L. Kiser Jr, D. R. Reinecke, and G. A. Kruger, "Thermoacoustic computed tomography using a conventional linear transducer array," *Medical physics*, vol. 30, no. 5, pp. 856–860, 2003.

[8] B. Huang, J. Xia, K. I. Maslov, and L. V. Wang, "Improving limited-view photoacoustic tomography with an acoustic reflector," *Journal of biomedical optics*, vol. 18, no. 11, p. 110505, 2013.

[9] S. Vilov, G. Godefroy, B. Arnal, and E. Bossy, "Photoacoustic fluctuation imaging: theory and application to blood flow imaging," *Optica*, vol. 7, pp. 1495–1505, Nov 2020.

[10] P. A. Bascom and R. S. Cobbold, "On a fractal packing approach for understanding ultrasonic backscattering from blood," *The Journal of the Acoustical Society of America*, vol. 98, no. 6, pp. 3040–3049, 1995.

[11] T. Chaigne, B. Arnal, S. Vilov, E. Bossy, and O. Katz, "Super-resolution photoacoustic imaging via flow-induced absorption fluctuations," *Optica*, vol. 4, no. 11, pp. 1397–1404, 2017.

[12] C. Demené, T. Deffieux, M. Pernot, B.-F. Osmanski, V. Biran, J.-L. Gennisson, L.-A. Sieu, A. Bergel, S. Franqui, J.-M. Correas, *et al.*, "Spatiotemporal clutter filtering of ultrafast ultrasound data highly increases doppler and fultrasound sensitivity," *IEEE transactions on medical imaging*, vol. 34, no. 11, pp. 2271–2285, 2015.

[13] G. Godefroy, B. Arnal, and E. Bossy, "Compensating for visibility artefacts in photoacoustic imaging with a deep learning approach providing prediction uncertainties," p. 100218.